

CoreEditor: Consistent 3D Editing via Correspondence-constrained Diffusion

Zhe Zhu, Honghua Chen, Peng Li, and Mingqiang Wei, *Senior Member, IEEE*

Abstract—Text-driven 3D editing seeks to modify 3D scenes according to textual descriptions, and most existing approaches tackle this by adapting pre-trained 2D image editors to multi-view inputs. However, without explicit control over multi-view information exchange, they often fail to maintain cross-view consistency, leading to insufficient edits and blurry details. We introduce CoreEditor, a novel framework for consistent text-to-3D editing. The key innovation is a correspondence-constrained attention mechanism that enforces precise interactions between pixels expected to remain consistent throughout the diffusion denoising process. Beyond relying solely on geometric alignment, we further incorporate semantic similarity estimated during denoising, enabling more reliable correspondence modeling and robust multi-view editing. In addition, we design a selective editing pipeline that allows users to choose preferred results from multiple candidates, offering greater flexibility and user control. Extensive experiments show that CoreEditor produces high-quality, 3D-consistent edits with sharper details, significantly outperforming prior methods.

Index Terms—3D Editing, Gaussian Splatting, Diffusion

I. INTRODUCTION

Recent advances in neural 3D representations, exemplified by NeRF [2] and Gaussian Splatting [3], have pushed the boundaries of photorealistic novel view synthesis, setting new benchmarks for fidelity and efficiency. Although these methods excel at reconstructing high-quality 3D scenes from multi-view images, once constructed, modifying these scenes to align with user preferences remains a challenging task. Developing such a 3D editing tool has become a critical research focus.

With the recent advances of diffusion-based text-to-image (T2I) models [4]–[6], most text-driven 3D editing approaches adapt these models to edit multi-view images in a zero-shot manner. However, the stochastic sampling process of diffusion models often induces cross-view inconsistencies, undermining their reliability for 3D scene optimization. The pioneering InstructNeRF2NeRF [7] addresses this issue via an iterative dataset update scheme, but suffers from slow convergence. Subsequent works [1], [8], [9] accelerate the process and enhance editing quality by jointly editing multiple views and enforcing inter-view alignment through strategies such as depth-conditioned ControlNet [6], cross-frame attention [10], and cross-view feature interpolation [9]. However, these strategies lack explicit constraints on multi-view information exchange, thereby compromising the consistency of image details. This

limitation becomes particularly pronounced under significant viewpoint variations and complex occlusions, often leading to inadequate edits and degraded details. As shown in Fig. 1, GaussCtrl [1] produces inconsistent and low-quality multi-view edits, resulting in rendering results with blurry texture.

In this paper, we propose CoreEditor to address these issues. CoreEditor achieves 3D consistency by integrating precise multi-view constraints into a pre-trained T2I diffusion model. It has been shown that, in a T2I model, tokens of different images can collaborate with each other in the attention module while still generating reasonable results [9]–[15]. Enlightened by this, our key idea is introducing a Correspondence-constrained Attention (CCA) in the diffusion U-Net, where image patches rendered from the same 3D point are constrained to interact with one another to improve visual consistency. Without the need for fine-tuning or re-training the diffusion model, the revised information flow direction of the attention module can significantly improve the consistency between multi-view generated content.

Despite its effectiveness, we identify two key challenges when directly applying CCA to diverse 3D editing: (1) When the camera distances between views are large, especially in some 360° scenes, the background image patches may have few geometrically corresponding patches in other views due to occlusion. The insufficient token count causes the attention process to become highly unstable, often leading to low-quality and over-saturated outputs (see Fig. 8). (2) When there is a significant disparity among per-view editing results, CCA tends to “average” these edits, resulting in unnatural edits.

To address the first one, we design a geometry and semantic co-supported approach to extract the multi-view correspondences. The key insight here is that semantically similar patches can also be involved in attention to improve consistency. As shown in Fig. 1 (a), although the left eye is occluded in the rightmost image, the accessible right eye is also expected to be visually consistent with the left one. Therefore, we are inspired to enrich the sparse geometric correspondences with semantic information. Specifically, in regions where geometric correspondences are unavailable, additional correspondences are calculated based on the diffusion feature similarity. With this comprehensive correspondence, CCA generates more plausible multi-view edits. Regarding the second problem, we introduce a selective editing pipeline, where users are allowed to select their preferred editing pattern from the per-view editing results. The selected edit is then injected into the diffusion model by a Reference Attention (RA). This approach ensures preliminary alignment of the global editing style, enabling CCA to focus solely on local consistency.

Z. Zhu, P. Li, and M. Wei are with the School of Computer Science and Technology, Nanjing University of Aeronautics and Astronautics, Nanjing, China. Email: {zhuzhe0619, pengli}@nuaa.edu.cn; mingqiang.wei@gmail.com.

H. Chen is with the School of Data Science, Lingnan University, Hong Kong, China. Email: chen honghuacn@gmail.com.

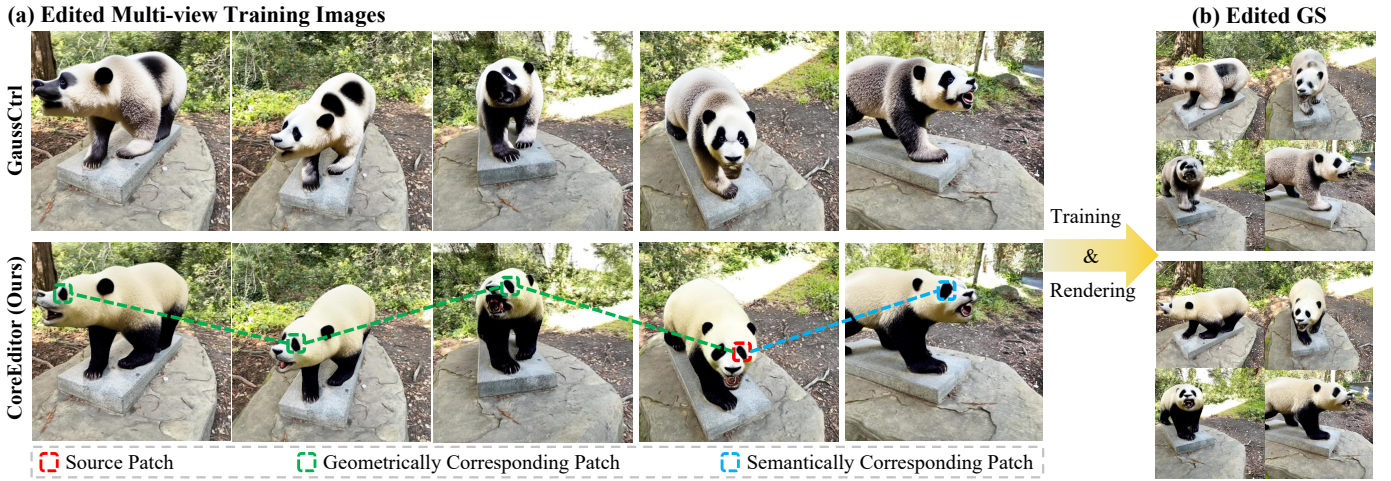


Fig. 1: **Key features of our method and visual comparison with the state-of-the-art GaussCtrl [1].** (a) Multi-view training image editing results. CoreEditor integrates geometric and semantic correspondences into the T2I diffusion model, achieving superior 3D-consistent edits compared with prior methods. (b) Rendered edited results. Leveraging consistent multi-view inputs, CoreEditor produces outputs with sharper textures and improved visual fidelity.

Moreover, CoreEditor can generate diverse yet faithful 3D edits by selecting different per-view editing patterns.

We conduct comprehensive experiments including various scenes and editing prompts. The results demonstrate that CoreEditor achieves superior results than its competitors in terms of multi-view consistency and editing quality. The main contributions of this work can be summarized as follows.

- We design a novel 3D editing method called CoreEditor, which significantly improves the multi-view consistency by a Correspondence-constrained Attention mechanism.
- We propose a geometry and semantic co-supported approach to build the multi-view correspondences, which significantly improves editing quality in complex scenes.
- We introduce a selective editing pipeline, which allows a flexible and user-centered 3D editing experience.

II. RELATED WORK

A. Text-driven 3D Editing

Early methods [16]–[18] primarily leverage vision-language models [19] for text-driven 3D stylization. However, their capabilities are often limited to modifying only the global style of the scene. Building upon the success of diffusion models, DreamFusion [20] introduces a score distillation sampling (SDS) loss for 3D generation from arbitrary text, which implicitly transfers prior knowledge from a pre-trained T2I model. The SDS loss has since been applied to 3D editing and personalization in several subsequent works [21]–[25].

InstructNerf2Nerf [7] is the first method to explicitly utilize a T2I model for this task. It addresses the issue of multi-view inconsistency by iteratively alternating between editing the training images and optimizing the 3D scene, which, however, results in a slow editing process. Following-up works improve the editing performance and speed by leveraging the explicit properties of 3D Gaussian splitting [26]–[29], latent space optimization [30]–[32], personalized editing [23], [33], [34], progressive editing [35], and 3D-aware fine-tuning of

the diffusion model [36]–[39]. Depth images are frequently used in recent methods to link different views. For example, VICA-NeRF [40] and DATENeRF [8] project edited images to other views using depth information. Among them, a prevalent approach involves propagating information between different views during multi-view joint editing. GaussCtrl [1] utilizes depth as guidance for ControlNet [6] and aligns the latent code of different views. DGE [9] applies cross-frame attention to edit key views, blending the edited features based on epipolar constraints. EditSplat [29] proposes a multi-view classifier-free guidance strategy to guide the diffusion model. Despite these advances, existing strategies often lack accurate constraints during the multi-view joint editing. Thereby, they typically fail to maintain precise 3D consistency. In contrast, we propose a novel correspondence-constrained attention mechanism, where only the corresponding tokens across views can communicate with each other. This enables a reliable information exchange across views, minimizing the introduction of irrelevant content and ensuring precise 3D consistency.

B. 3D-aware Diffusion Model

Extensive efforts have been made to introduce 3D awareness into pre-trained T2I diffusion models, transforming them into multi-view generators. The pioneering work Zero-1-to-3 [41] incorporates relative pose as an additional condition to generate novel views from a single-view observation. Building on this, SyncDreamer [42] connects corresponding pixels through a feature volume. MVDream [43] and Imagedream [44] process all pixels across multi-view images together, significantly increasing computational complexity. To allow for precise control and reduce computational costs, recent methods integrate 3D constraints [45]–[49] and camera positional embedding [50] into the attention module. Our CoreEditor shares similarities with these approaches in extending a pre-trained diffusion model to a multi-view network. However, unlike these methods, which introduce a large number of trainable

parameters and require extensive fine-tuning, our method can be seamlessly integrated into existing diffusion models in a zero-shot manner.

III. METHOD

A. Preliminaries

3D Gaussian Splatting. Our method adopts Gaussian Splatting (GS) [3] as the 3D representation. In GS, a 3D scene is represented as a collection of Gaussian primitives, each characterized by its center coordinate μ , covariance matrix Σ , opacity σ , and color c represented by spherical harmonic coefficients. To enable real-time rendering, GS employs a splatting rendering approach, where the color is computed by blending the contributions of Gaussians projected onto that pixel. Similar to NeRF [2], GS is also capable of reconstructing depth by computing the weighted average of the distance values of the projected Gaussians.

Latent Diffusion Model. Recently, latent diffusion model [51] has emerged as a dominant architecture for image generation. It reduces computational overhead by compressing images into a low-dimensional latent space, where both the forward and backward diffusion processes [4], [52] are performed. The denoising network employs a U-Net [53] architecture, with each layer consisting of a self-attention (SA) and a text cross-attention (CA) module.

DDIM Inversion for Image Editing. DDIM inversion [52] enables the reversal of an image to its corresponding noise representation in diffusion space. A typical image editing workflow involves first inverting the image to noise Z^T , then regenerating the edited version using the inverted noise and a target text prompt. To preserve the original layout, additional constraints, such as attention feature replacement [11], [54], are often applied during the editing process.

B. Overview: Selective Editing Pipeline

Given a 3D GS model \mathcal{G} and a text prompt T , we propose CoreEditor to modify \mathcal{G} such that it faithfully aligns with T . Ideally, if multi-view consistent edited images can be obtained, \mathcal{G} can be updated accordingly to achieve high-quality 3D edits. As shown in Fig. 2, CoreEditor ensures consistent multi-view editing through a re-designed denoising U-Net architecture. Specifically, after rendering multi-view source images $\mathcal{I} = \{I_i\}_{i=1}^N$ and depth maps $\mathcal{D} = \{D_i\}_{i=1}^N$ from N views, CoreEditor performs the editing in two main steps:

(1) We first align multi-view edits towards a user-selected style. In particular, each image in \mathcal{I} is firstly edited using a standard inversion-based approach, during which we save the intermediate diffusion features at each layer. After the editing process, users can select their preferred result, I^r , which serves as the reference edit for the following steps. The corresponding feature F^r is then injected into the subsequent steps through Reference Attention (RA) (Sec. III-C).

(2) In the second step, we incorporate multi-view constraints into the diffusion process and jointly edit images in \mathcal{I} to an image set \mathcal{I}^e with consistent local details. In detail, \mathcal{I} and \mathcal{D} are used to build geometry and semantic co-supported correspondence (Sec. III-D). Those correspondences are integrated

by introducing a Correspondence-constrained Attention (CCA) module (Sec. III-E) in the U-Net. With the modified diffusion model, we use the inversion-based editing method to get \mathcal{I}^e , which is then used to optimize \mathcal{G} .

During the above process, the diffusion model is kept frozen, without introducing any additional training.

C. Reference Attention (RA)

Since edited results for the same prompt can be completely different across views, posing difficulties in producing high-quality edits while keeping consistency between them, we allow the users to select their preferred editing pattern, which guides the entire editing process through attention feature injection. Specifically, we modify the SA module within the diffusion backward process, transforming it into an RA module. As presented in Fig. 3, compared with SA, the diffusion feature F^r of I^r serves as an additional key and value in RA, thus facilitating the alignment of the editing style. Given the multi-view input features $\mathcal{F} = \{F_i\}_{i=1}^N$ in the reference attention module, the output feature Z_i for the i -th view is computed as:

$$Z_i = \lambda \cdot \text{softmax} \left(\frac{W_q F_i (W_k F^r)^\top}{\sqrt{d_k}} \right) W_v F^r + (1 - \lambda) \cdot \text{softmax} \left(\frac{W_q F_i (W_k F_i)^\top}{\sqrt{d}} \right) W_v F_i \quad (1)$$

where W_q , W_k , and W_v are projection matrices in the attention module, and $\lambda \in [0, 1]$ is a coefficient that modulates the weighting of the reference and original attention terms. After injecting I^r , the global editing patterns have been aligned, significantly reducing the solution space for consistent results. **Furthermore, manual selection can also be automated through the human preference predictor [55], establishing a fully automatic workflow (See results in Sec. IV-D).**

D. Geometry and Semantic Co-supported Correspondence

We first build image correspondence relationships between views to serve as precise 3D constraints for the diffusion model. For a pixel coordinate $P = (x_s, y_s)$ in the s -th view, our goal is to find its correspondences $\mathcal{C} = \{(x_i, y_i) \mid i = 1, 2, \dots, N, i \neq s\}$ in the remaining $N - 1$ views. Geometric correspondence can be directly derived from the depth maps \mathcal{D} . The geometrically corresponding pixel (x_a, y_a) of P in a target view a is obtained as:

$$(x_a, y_a) = \text{Proj}(\text{BackProj}((x_s, y_s), D_s, K, E_s), K, E_a) \quad (2)$$

where K , E_s , and E_a are the intrinsic and extrinsic camera parameters of views s and a . In this process, P is first back-projected into 3D space using the depth D_s of this view, then re-projected to the target view a to obtain its corresponding pixel location. To handle potential occlusions, we compute a re-projection error to construct a correspondence mask $M = \{m_i \mid m_i \in \{0, 1\}, i = 1, 2, \dots, N, i \neq s\}$, filtering out unreliable matches.

However, as discussed in Sec. I, certain pixels should exhibit visual consistency across views even without valid geometric

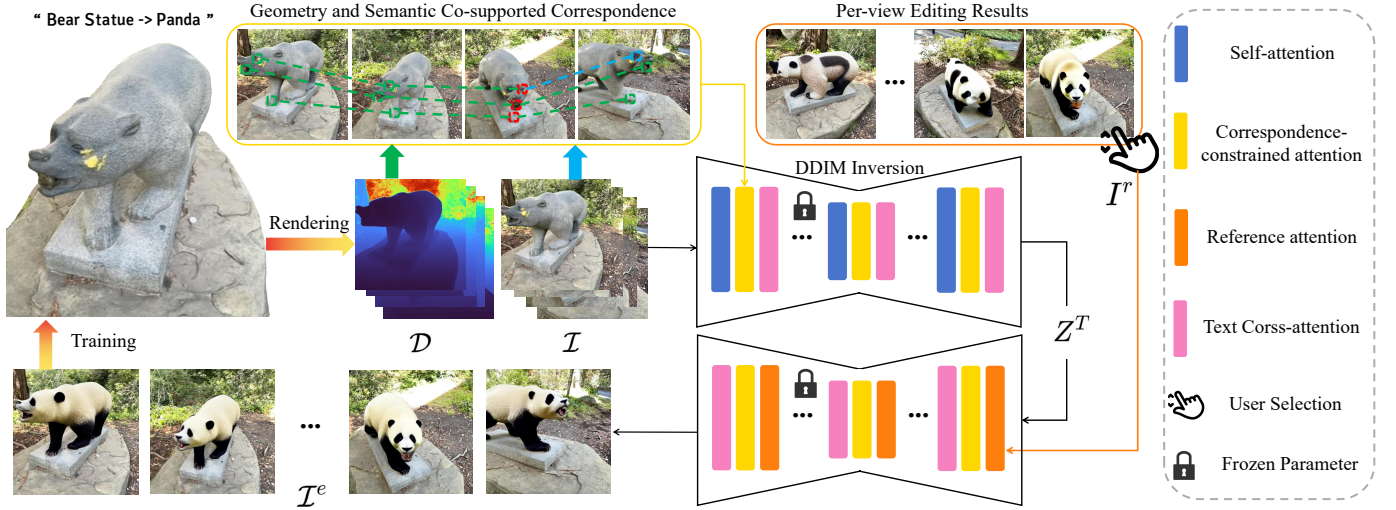


Fig. 2: **Overview of CoreEditor.** Our method edits the rendered multi-view images (\mathcal{I}) into a consistent image set \mathcal{I}^e , which is then used to update the original GS model. The process ensures 3D consistency through two key steps: (1) Once the user selects a preferred edit, I^r , we integrate its pattern into the diffusion model using Reference Attention. (2) After the geometry and semantic co-supported correspondence set has been established, we inject it into the diffusion model by Correspondence-constrained Attention.

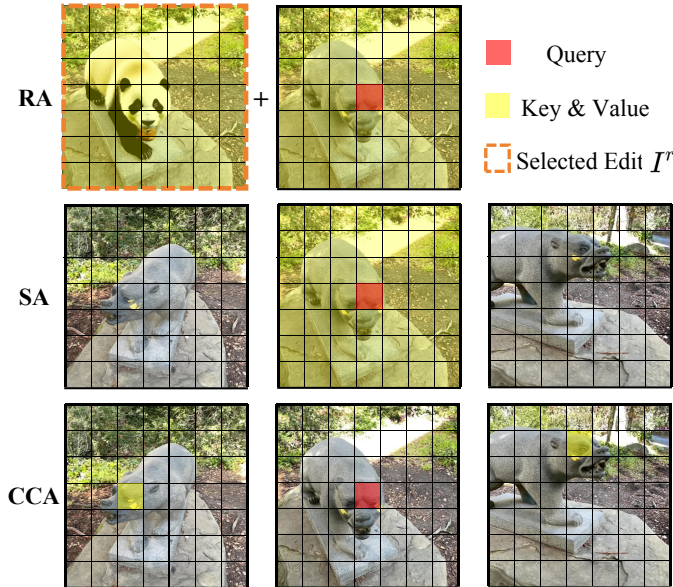


Fig. 3: Difference between the calculation of RA, SA, and CCA. Compared with the original SA, RA regards the selected edit as an additional set of key and value. To improve local consistency, CCA enforces an image patch token to only interact with the corresponding patches in other views.

correspondence. These implicit relationships can enrich the sparse geometric correspondence and stabilize the attention mechanism. Inspired by recent work demonstrating emergent correspondence in image diffusion models [56], we obtain additional semantic correspondence based on diffusion features. To be specific, we apply a single forward and backward step of DDPM to \mathcal{I} and extract the last-layer feature maps $\mathcal{H} = \{H_i\}_{i=1}^N$ output by the U-Net. Then, for a target view b lacking valid geometric correspondence for P , We define its

corresponding pixel (x_b, y_b) as the location with the highest feature cosine similarity:

$$(x_b, y_b) = \operatorname{argmax}_{(x,y)} \frac{H_s(x_s, y_s) \cdot H_b(x, y)}{\|H_s(x_s, y_s)\| \|H_b(x, y)\|} \quad (3)$$

Since valuable information exists only in some specific target views, we only use semantic correspondences with the highest cosine similarity exceeding a threshold value β . Other semantic correspondences are retained masked. Here, to avoid additional hyper-parameter tuning, we typically set β to 0.9, which performs well across various scenes. Finally, a comprehensive correspondence set \mathcal{C} has been established, accompanied by a mask M indicating the validity of each correspondence.

E. Correspondence-constrained Attention (CCA)

We then incorporate \mathcal{C} into the diffusion U-Net through the proposed CCA module. Detailedly, in both the DDIM inversion and the denoising backward process, a CCA is placed after each self-attention/reference attention module. Given the multi-view features $\mathcal{Z} = \{Z_i\}_{i=1}^N$ output by self/reference attention modules, the output token P from CCA can be calculated as:

$$\begin{aligned} Q &= Z_s(x_s, y_s), \\ K &= V = \{Z_i(\mathcal{C}[i]) \mid i = 1, 2, \dots, N\}, \\ P' &= \operatorname{softmax} \left(\frac{QK^\top}{\sqrt{d}} + M' \right) V \end{aligned} \quad (4)$$

Here, we do not introduce additional parameters for re-projecting the latent; rather, we alter the direction of the information flow and perform the attention calculation once more. Fig. 3 illustrates how CCA works: It constrains P to only interact with image tokens belonging to \mathcal{C} instead of querying image tokens within the source view. Meanwhile, we filter out correspondences that are identified as invalid

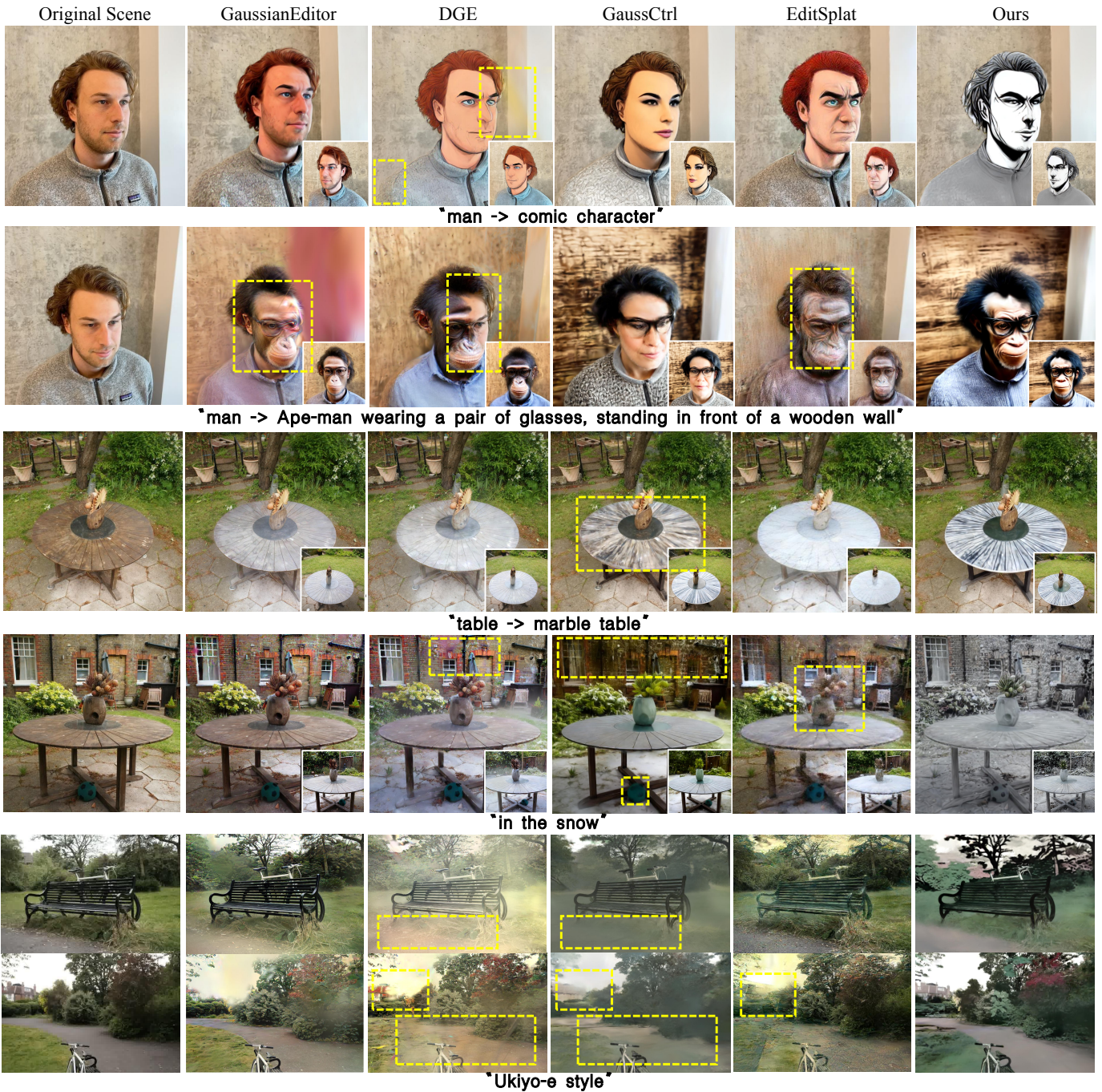


Fig. 4: Visual comparison with state-of-the-art methods [1], [9], [27], [29] in the “face”, “garden”, and “bicycle” scenes. We provide results rendered from two views for each edited scene. Blurry regions are highlighted with yellow dash boxes.

in Sec. III-D by extending M to an attention mask M' . Without any need for fine-tuning the diffusion model, the precise interaction between views significantly improves the multi-view consistency, thereby making the diffusion model a high-quality 3D editor.

IV. EXPERIMENT

A. Experimental Setup

Implementation Details. We adopt Splatfacto as the 3D representation, a modified version of Gaussian Splatting [3],

implemented within the Nerfstudio library [57]. For the text-to-image (T2I) model, we use Stable Diffusion v1.5 [51] combined with its corresponding depth-conditioned ControlNet [6], implemented in the Diffusers library [58]. For local editing, where the irrelevant background is expected to remain unchanged, we utilize Lang-SAM [59] to generate masks for the edited images, filtering out the background. In all the experiments, we manually select I' from the per-view edits. Then, the proposed multi-view editing is applied with 500 steps of GS optimization. The commonly used L1 and LPIPS [60] losses are applied as the objective function during

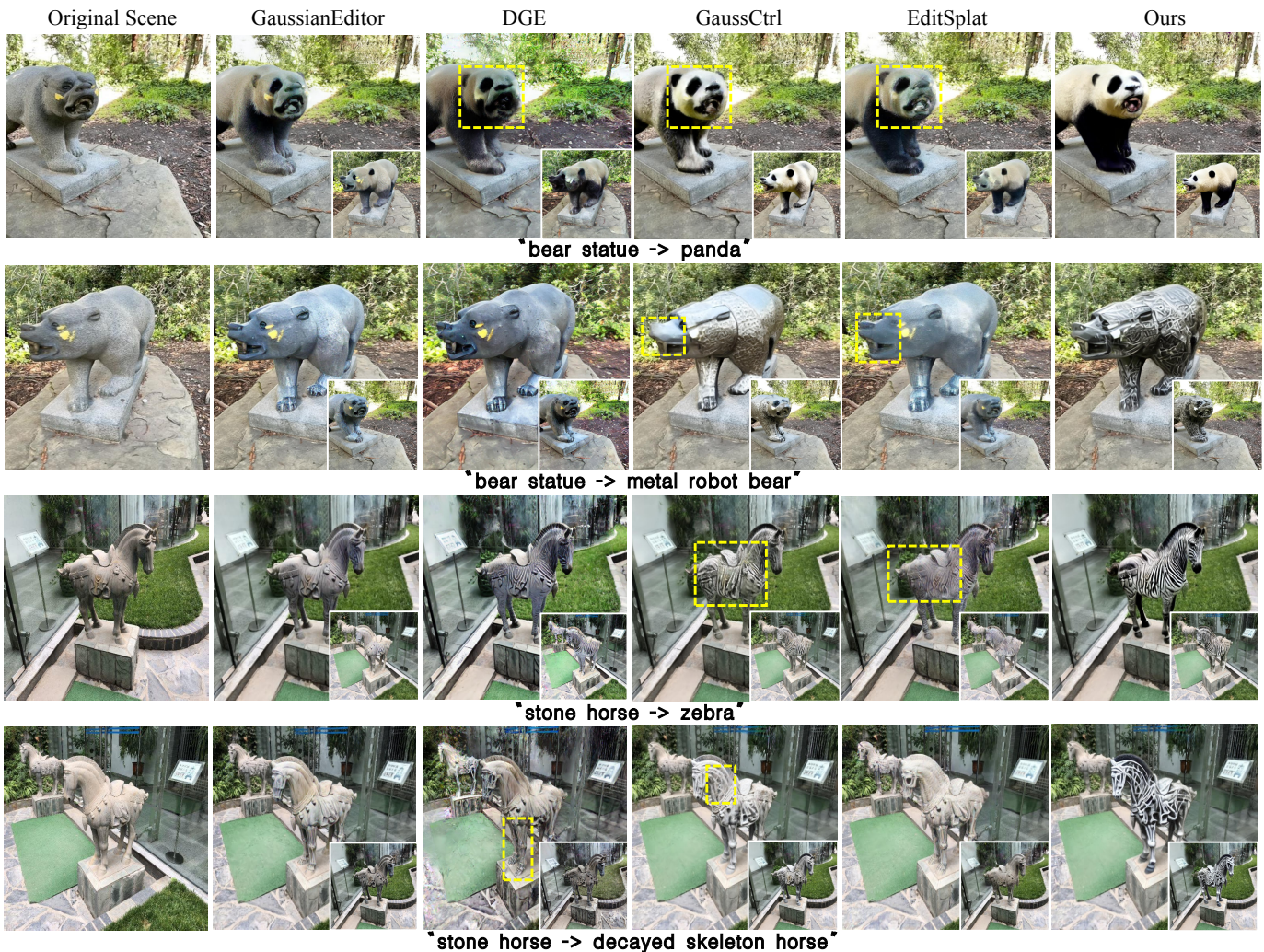


Fig. 5: Visual comparison with state-of-the-art methods [1], [9], [27], [29] in the “bear” and “stone horse” scenes. We provide results rendered from two views for each edited scene. Blurry regions are highlighted with yellow dash boxes.

the GS optimization. The number of multi-view images N is set to 20, randomly sampled in the training set. During the DDIM inversion and backward denoising process, we use 20 diffusion steps. For scene stylization prompts, λ is set to 0.3. For other prompts, such as human character editing, which exhibit high variability and may generate vastly different styles, we employ a higher λ value of 0.5. This ensures that the selected edit is consistently replicated across different views. For all scenes, β is set as 0.9.

Data. We evaluate CoreEditor on seven scenes from Instruct-NeRF2NeRF [7], Mip-NeRF 360 [61], BlendMVS [62], and NerfStudio [57], including the “bear” and “face” scenes from [7], the “bicycle” and “garden” scenes from [61], the “stone horse” and “dinosaur” scenes from [62], and the “dozer” scene from [57]. The performance of our method is evaluated across a total of 20 challenging prompts, covering tasks such as local editing, global stylization, and human character modification.

Baselines. We compare CoreEditor against four state-of-the-art GS-based 3D editing methods: GaussianEditor [27], DGE [9], GaussCtrl [1], and EditSplat [29]. GaussianEditor employs the iterative dataset update strategy introduced in [7],

while DGE, GaussCtrl and EditSplat adopt a joint multi-view image editing approach similar to our method.

B. Qualitative Results

We present the qualitative comparison in Fig. 4 and Fig. 5, showcasing editing results from two viewpoints. Compared to state-of-the-art methods [1], [9], [27], [29], CoreEditor achieves better performance in producing vivid 3D edits that closely adhere to the text prompts. This advancement is largely due to the multi-view consistent 2D edits.

Based on the results, we can conclude that the inconsistency issues of other methods are mainly reflected in two aspects: (1) **Incomplete Editing:** When the edited training images are highly inconsistent, the resulting 3d scenes often exhibit insufficient visual change. For instance, GaussianEditor and EditSplat fail to modify the original GS model in the “decayed skeleton horse” cases in Fig. 5. GaussCtrl exhibits similar limitations, as evidenced by its inability to successfully transform the human subject into an ape-man in Fig. 4. (2) **Degraded Rendering Quality:** In some scenarios, although existing methods can partially achieve the target edits, they

TABLE I: Quantitative comparison with recent methods [1], [9], [27], [29] (CLIP_{sim} : CLIP similarity scores, CLIP_{dir} : CLIP directional similarity scores, Met3R values [63], and User study voting rates).

Methods	CLIP Metrics		Met3R↓	User Study	
	CLIP _{sim} ↑	CLIP _{dir} ↑		Quality↑	Consistency↑
GaussianEditor [27]	0.244	0.086	-	7.0%	8.8%
DGE [9]	0.259	0.123	0.390	14.6%	15.0%
GaussCtrl [1]	0.257	0.128	0.372	16.2%	14.8%
EditSplat [29]	0.261	0.130	0.336	17.0%	19.4%
Ours	0.270	0.145	0.281	45.2%	42.0%

still produce locally inconsistent multi-view edits, resulting in Blurry renderings with noticeable artifacts (highlighted by yellow dashed boxes in Fig. 4 and Fig. 5). Specifically, for the stylization of 360° scenes, such as the “snow” and “Ukiyo-e” cases in Fig. 4, the inconsistency introduces foggy artifacts that significantly degrade visual quality. Similarly, in the “panda” case in Fig. 5, all the competitors produce vague panda faces. In contrast, CoreEditor, equipped with the proposed CAA module and selective editing pipeline, effectively aligns multi-view edits at both global and local levels, significantly outperforming existing methods. Besides, we also present a qualitative comparison with GaussCtrl [1] using a free-viewpoint rendering video in the supplemental material. The comparison highlights that CoreEditor produces more faithful edits while substantially mitigating flickering artifacts. This further underscores the superior consistency brought by our method.

C. Quantitative Results

The quantitative comparison with baseline methods is summarized in Tab. I. Following the previous practice [1], [7], [9], we evaluate the performance using two CLIP-based metrics computed on rendered images: the CLIP similarity score and the CLIP directional similarity score [7]. The CLIP similarity score measures the degree of alignment between the edited images and the target text prompt, while the CLIP directional similarity score assesses how well the visual changes correspond to the semantic changes implied by the text. As shown in Tab. I, CoreEditor consistently outperforms all baseline methods across both metrics, highlighting its superior ability to generate edits that are semantically faithful to the text prompt. To quantitatively evaluate the 3D consistency of CoreEditor, we employ the recently proposed Met3R metric [63], which measures feature similarity between view-warped DINO [64] features. We compute the Met3R values on the edited multi-view training images generated by DGE, GaussCtrl, EditSplat and our method. GaussianEditor is excluded from this comparison as it does not support joint multi-view image editing. The results demonstrate that CoreEditor significantly improves 3D consistency compared to baseline methods through the proposed techniques. Moreover, given the inherently subjective nature of 3D editing, we validate our method through a user study involving 50 participants and 10 editing prompts. Given the source scene, editing prompts, and the rendered videos of each method, participants were asked to select the best method based on two criteria, respectively: (1) Overall visual quality

and (2) 3D consistency (mainly based on the frequency of flickering artifacts in rendered videos). The user voting rates in Tab. I indicate a clear preference for CoreEditor’s outputs, further corroborating the advantages of our approach from a human perceptual perspective.

Efficiency Analysis. Leveraging its zero-shot diffusion design, CoreEditor accomplishes multi-view joint editing with only 18 GB of GPU memory under default settings. It edits scene in about 8 minutes—faster than EditSplat (12 min) and GaussianEditor (25 min), comparable to GaussCtrl (10 min), and only slightly slower than the fastest baseline, DGE (5 min). Crucially, CoreEditor achieves these results while delivering substantial and consistent gains in editing quality, offering a favorable balance between accuracy and efficiency.

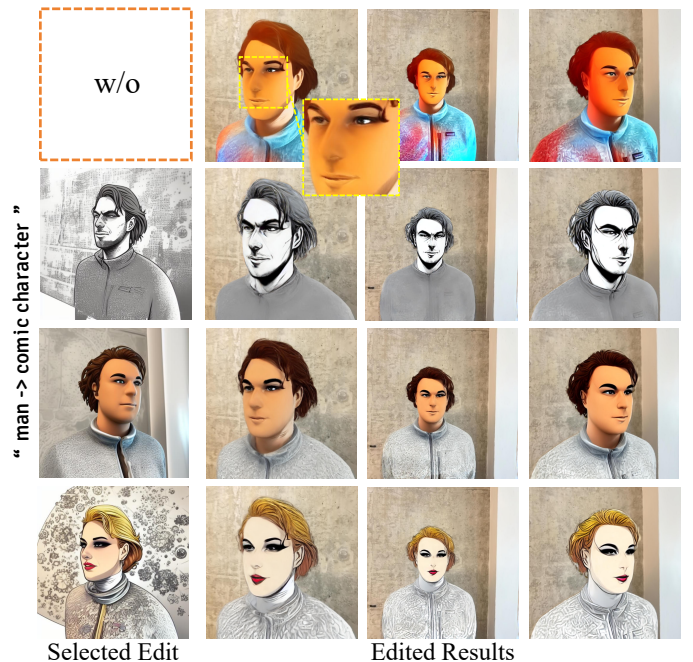


Fig. 6: Results with different per-view edits I^r selected.

D. Ablation Study

We ablate the main components of CoreEditor by presenting quantitative and qualitative comparisons.

Effect of Selective Editing Pipeline. In Fig. 6, we first evaluate the impact of selective editing by removing the selection process and disabling the RA module. As shown in the first row, rendering results exhibit unnatural color distribution



Fig. 7: Edited training images of [1] and different ablation variants for the “joker” prompt of the “face” scene. The selected edit I^r is highlighted using a dash box. Only CoreEditor ensures faithful propagation of the selected edit while maintaining 3D consistency across views.

when the selection stage is omitted. This issue arises because the per-view edits for the “comic character” prompt exhibit significant variations. Without selective editing, relying solely on a multi-view constraint like CAA leads to the blending of these highly varied edits, ultimately resulting in unnatural colors. The decreased CLIP metrics in Tab. II also indicate misaligned edits with the text prompts when the selective editing is removed. To address this, we pre-align the global editing styles with the selected reference edit. As demonstrated in the subsequent rows of Fig. 6, selecting different I^r enables CoreEditor to produce 3D edits with entirely distinct visual patterns. This flexibility facilitates a highly adaptable and user-centric editing process, empowering users to tailor edits more effectively to their desired visual styles or specific preferences. **Manual vs. Automatic Selection.** While the selective editing design provides a user-centered editing experience, it introduces an additional manual step that may reduce workflow efficiency. To enable fully automatic editing within our CoreEditor, we replace manual selection with the ImageReward model [55], which evaluates generated images based on their alignment with the text prompt. Specifically, for a given target prompt, we rank all per-view edits using ImageReward and select the top-ranked edit as the reference. The quantitative results in Tab. II show that the performance of CoreEditor remains comparable regardless of whether manual or automatic selection is used. This robustness confirms that our selective editing framework flexibly accommodates both manual and automatic selection modes. Furthermore, to ensure a comprehensive comparison with state-of-the-art methods, we integrate the RA module (with both manual and automatic selection) into GaussCtrl [1] in Tab. II. While the selective editing strategy improves GaussCtrl’s performance, it still exhibits limitations in generating text-faithful edits. This is clearly demonstrated by its inferior CLIP scores and higher

TABLE II: Effect of the selective editing pipeline.

Methods	CLIP _{sim} ↑	CLIP _{dir} ↑	Met3R ↓
GaussCtrl [1]	0.257	0.128	0.372
[1] + RA (Automatic)	0.258	0.129	0.357
[1] + RA (Manual)	0.260	0.132	0.352
Ours w/o RA	0.258	0.133	0.292
Ours (Automatic)	0.267	0.145	0.283
Ours (Manual)	0.270	0.145	0.281

Met3R values compared to our approach, indicating that without consistency provided by our CCA, GaussCtrl cannot achieve edits that are faithfully aligned with prompts.

Effect of CCA. In Tab. III, the Met3R value significantly increases when CCA is disabled, indicating the importance of CCA for ensuring multi-view consistency. In Fig. 7, we evaluate the effectiveness of the CCA module by comparing edited training images produced by different variants. In the first row, the standard DDIM inversion-based editor is applied to edit multi-view images independently, view by view. Without any multi-view fusion strategy, the per-view edits exhibit significant inconsistency. Next, as shown in the third row, we introduce the RA module to the basic 2D editor by selecting a reference edit I^r (highlighted with a dash box). However, in the absence of a precise multi-view constraint, the RA variant is only capable of aligning visual patterns at a global level, failing to maintain consistency in local image details. Finally, we incorporate the proposed CCA module into the diffusion model. With this precise multi-view constraint, the diffusion model effectively links edits across views, producing results with high-level consistency in both global patterns and local details, as demonstrated in the last row.

Effect of Co-supported Correspondence. We evaluate the



Fig. 8: Ablation study of the co-supported correspondence. (a) Semantic correspondences obtained through the diffusion feature for the “garden” scene. Invalid correspondences filtered out by β are marked as yellow. (b) Edited training images of different ablation variants. Without the semantic correspondence, the output images become unnatural and fail to preserve the original layout structure due to the insufficient attention token count.

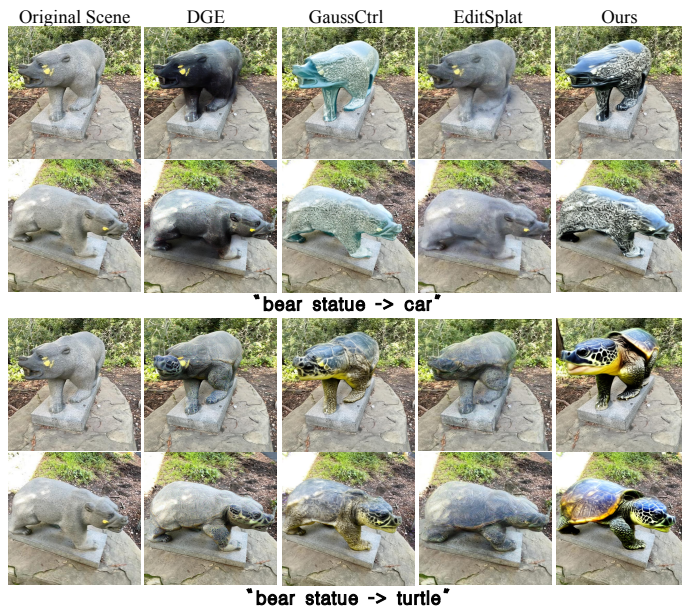


Fig. 9: Qualitative comparison with recent methods [1], [9], [29] on prompts requiring shape changes.

co-supported correspondence by analyzing the 2D editing results of different variants, as shown in Fig. 8. We first visualize the semantic correspondences derived from diffusion

TABLE III: Effect of the Correspondence-constraint Attention.

Methods	CLIP _{sim} ↑	CLIP _{dir} ↑	Met3R ↓
w/o CAA	0.250	0.124	0.378
w/o Geometric	0.245	0.118	0.351
w/o Semantic	0.266	0.128	0.294
Ours	0.270	0.145	0.281

TABLE IV: Effect of varying β .

Methods	CLIP _{sim} ↑	CLIP _{dir} ↑	Met3R ↓
w/o β	0.257	0.133	0.297
$\beta = 0.8$	0.265	0.136	0.292
$\beta = 0.85$	0.271	0.142	0.289
$\beta = 0.9$	0.270	0.145	0.281
$\beta = 0.95$	0.266	0.137	0.290

features, which can accurately capture corresponding patches with similar semantic meanings, as demonstrated in Fig. 8 (a). Then, we assess the impact of removing semantic correspondences while relying solely on geometric information. In 360° scenes like the “garden”, geometric correspondences for background pixels are sparse due to the training data focusing on central objects. As illustrated in the first column of Fig. 8 (b), the lack of tokens destabilizes the attention mechanism, resulting in distorted background and over-saturated colors. This degraded visual quality can also be reflected by the

decreased CLIP metrics in Tab. III. Next, we replace all geometric correspondences with semantic ones. As shown in the second column of Fig. 8 (b) and the increased Met3R value in Tab. III, this substitution leads to incomplete and inconsistent edits, as the well-reconstructed geometric correspondences are more accurate for central objects.

Effect of β . We firstly analyze the effect of the threshold β by disabling it. Fig. 8 (a) indicates that some views lack patches with highly similar semantic meanings, and including such tokens may introduce noisy information, as evidenced by the excessive noise in the fourth column of Fig. 8 (b). Results in the first row of Tab. III further quantify the effect of β . We also ablate the value of β in Tab. III and find that CoreEditor achieves the best performance when $\beta = 0.9$.

E. Limitations

Similar to recent methods [1], [8], [29], [40], CoreEditor leverages the original scene geometry to improve 3D consistency. As a result, our approach is limited in its ability to significantly modify scene geometry. As illustrated by the failure case in the first row of Fig. 9, both CoreEditor and other methods fail to transform the bear statue into a car. However, unlike methods such as [8], [40], which directly warp pixels based on depth maps, CoreEditor enforces correspondence-based constraints within the diffusion latent space, where the minimal patch size is 8×8 . This design makes CoreEditor more robust to depth errors and allows it to handle target edits with shapes that differ from the original models. The second row of Fig. 9 demonstrates that, for prompts requiring shape modification, our method surpasses baseline methods [1], [9], [29] by enabling greater geometric changes while maintaining high-quality rendering, thanks to our consistent 2D edits.

V. CONCLUSION

We propose CoreEditor, a novel framework for text-driven 3D editing that significantly enhances the quality of edited 3D scenes by improving consistency during multi-view editing. At the heart of our method is the correspondence-constrained attention module, which enforces interactions between image patches that should remain consistent within the diffusion model. To handle complex scenes with the proposed attention module, we introduce a geometry and semantic co-supported strategy to extract comprehensive correspondences, ensuring robust multi-view editing. Additionally, we design a selective editing pipeline that empowers users to choose their preferred edits from multiple candidates, enabling a highly flexible and user-centric editing process. Extensive experiments on widely-used datasets demonstrate that CoreEditor achieves state-of-the-art editing performance. These results highlight its effectiveness in extending 2D diffusion models to consistent 3D editing, representing an important step toward more flexible and controllable 3D AIGC.

REFERENCES

- [1] J. Wu, J.-W. Bian, X. Li, G. Wang, I. Reid, P. Torr, and V. A. Prisacariu, "Gaussctrl: Multi-view consistent text-driven 3d gaussian splatting editing," in *European Conference on Computer Vision*, 2024, pp. 55–71.
- [2] B. Mildenhall, P. P. Srinivasan, M. Tancik, J. T. Barron, R. Ramamoorthi, and R. Ng, "Nerf: Representing scenes as neural radiance fields for view synthesis," *Communications of the ACM*, vol. 65, no. 1, pp. 99–106, 2021.
- [3] B. Kerbl, G. Kopanas, T. Leimkühler, and G. Drettakis, "3d gaussian splatting for real-time radiance field rendering," *ACM Trans. Graph.*, vol. 42, no. 4, pp. 139–1, 2023.
- [4] J. Ho, A. Jain, and P. Abbeel, "Denoising diffusion probabilistic models," *Advances in neural information processing systems*, vol. 33, pp. 6840–6851, 2020.
- [5] R. Rombach, A. Blattmann, D. Lorenz, P. Esser, and B. Ommer, "High-resolution image synthesis with latent diffusion models," in *Proceedings of the IEEE/CVF conference on computer vision and pattern recognition*, 2022, pp. 10 684–10 695.
- [6] L. Zhang, A. Rao, and M. Agrawala, "Adding conditional control to text-to-image diffusion models," in *Proceedings of the IEEE/CVF International Conference on Computer Vision*, 2023, pp. 3836–3847.
- [7] A. Haque, M. Tancik, A. A. Efros, A. Holynski, and A. Kanazawa, "Instruct-nerf2nerf: Editing 3d scenes with instructions," in *Proceedings of the IEEE/CVF International Conference on Computer Vision*, 2023, pp. 19 740–19 750.
- [8] S. Rojas, J. Philip, K. Zhang, S. Bi, F. Luan, B. Ghanem, and K. Sunkavalli, "Datenerf: Depth-aware text-based editing of nerfs," in *European Conference on Computer Vision*, 2024, pp. 267–284.
- [9] M. Chen, I. Laina, and A. Vedaldi, "Dge: Direct gaussian 3d editing by consistent multi-view editing," in *European Conference on Computer Vision*, 2024, pp. 74–92.
- [10] J. Z. Wu, Y. Ge, X. Wang, S. W. Lei, Y. Gu, Y. Shi, W. Hsu, Y. Shan, X. Qie, and M. Z. Shou, "Tune-a-video: One-shot tuning of image diffusion models for text-to-video generation," in *Proceedings of the IEEE/CVF International Conference on Computer Vision*, 2023, pp. 7623–7633.
- [11] N. Tumanyan, M. Geyer, S. Bagon, and T. Dekel, "Plug-and-play diffusion features for text-driven image-to-image translation," in *Proceedings of the IEEE/CVF Conference on Computer Vision and Pattern Recognition*, 2023, pp. 1921–1930.
- [12] M. Cao, X. Wang, Z. Qi, Y. Shan, X. Qie, and Y. Zheng, "Masactrl: Tuning-free mutual self-attention control for consistent image synthesis and editing," in *Proceedings of the IEEE/CVF International Conference on Computer Vision*, 2023, pp. 22 560–22 570.
- [13] Y. Cong, M. Xu, C. Simon, S. Chen, J. Ren, Y. Xie, J.-M. Perez-Rua, B. Rosenhahn, T. Xiang, and S. He, "Flatten: optical flow-guided attention for consistent text-to-video editing," *arXiv preprint arXiv:2310.05922*, 2023.
- [14] J. Nam, H. Kim, D. Lee, S. Jin, S. Kim, and S. Chang, "Dreammatcher: Appearance matching self-attention for semantically-consistent text-to-image personalization," in *Proceedings of the IEEE/CVF Conference on Computer Vision and Pattern Recognition*, 2024, pp. 8100–8110.
- [15] Y. Zhou, D. Zhou, M.-M. Cheng, J. Feng, and Q. Hou, "Storydiffusion: Consistent self-attention for long-range image and video generation," 2024.
- [16] O. Michel, R. Bar-On, R. Liu, S. Benaim, and R. Hanocka, "Text2mesh: Text-driven neural stylization for meshes," in *Proceedings of the IEEE/CVF Conference on Computer Vision and Pattern Recognition*, 2022, pp. 13 492–13 502.
- [17] C. Wang, M. Chai, M. He, D. Chen, and J. Liao, "Clip-nerf: Text-and-image driven manipulation of neural radiance fields," in *Proceedings of the IEEE/CVF Conference on Computer Vision and Pattern Recognition*, 2022, pp. 3835–3844.
- [18] C. Wang, R. Jiang, M. Chai, M. He, D. Chen, and J. Liao, "Nerf-art: Text-driven neural radiance fields stylization," *IEEE Transactions on Visualization and Computer Graphics*, vol. 30, no. 8, pp. 4983–4996, 2024.
- [19] A. Radford, J. W. Kim, C. Hallacy, A. Ramesh, G. Goh, S. Agarwal, G. Sastry, A. Askell, P. Mishkin, J. Clark *et al.*, "Learning transferable visual models from natural language supervision," in *International conference on machine learning*, 2021, pp. 8748–8763.
- [20] B. Poole, A. Jain, J. T. Barron, and B. Mildenhall, "Dreamfusion: Text-to-3d using 2d diffusion," in *The Eleventh International Conference on Learning Representations*, 2023.
- [21] E. Sella, G. Fiebelman, P. Hedman, and H. Averbuch-Elor, "Vox-e: Text-guided voxel editing of 3d objects," in *Proceedings of the IEEE/CVF International Conference on Computer Vision*, 2023, pp. 430–440.
- [22] J. Zhuang, C. Wang, L. Lin, L. Liu, and G. Li, "Dreameditor: Text-driven 3d scene editing with neural fields," in *SIGGRAPH Asia 2023 Conference Papers*, 2023, pp. 1–10.

- [23] J. Zhuang, D. Kang, Y.-P. Cao, G. Li, L. Lin, and Y. Shan, “Tip-editor: An accurate 3d editor following both text-prompts and image-prompts,” *ACM Transactions on Graphics (TOG)*, vol. 43, no. 4, pp. 1–12, 2024.
- [24] A. Mirzaei, T. Aumentado-Armstrong, M. A. Brubaker, J. Kelly, A. Levinstein, K. G. Derpanis, and I. Gilitschenski, “Watch your steps: Local image and scene editing by text instructions,” in *European Conference on Computer Vision*, 2024, pp. 111–129.
- [25] H. Chen, C. C. Loy, and X. Pan, “Mvip-nerf: Multi-view 3d inpainting on nerf scenes via diffusion prior,” in *Proceedings of the IEEE/CVF Conference on Computer Vision and Pattern Recognition*, 2024, pp. 5344–5353.
- [26] J. Wang, J. Fang, X. Zhang, L. Xie, and Q. Tian, “Gaussianeditor: Editing 3d gaussians delicately with text instructions,” in *Proceedings of the IEEE/CVF Conference on Computer Vision and Pattern Recognition*, 2024, pp. 20902–20911.
- [27] Y. Chen, Z. Chen, C. Zhang, F. Wang, X. Yang, Y. Wang, Z. Cai, L. Yang, H. Liu, and G. Lin, “Gaussianeditor: Swift and controllable 3d editing with gaussian splatting,” in *Proceedings of the IEEE/CVF Conference on Computer Vision and Pattern Recognition*, 2024, pp. 21476–21485.
- [28] Y. Wang, X. Yi, Z. Wu, N. Zhao, L. Chen, and H. Zhang, “View-consistent 3d editing with gaussian splatting,” in *European Conference on Computer Vision*, 2024, pp. 404–420.
- [29] D. I. Lee, H. Park, J. Seo, E. Park, H. Park, H. D. Baek, S. Shin, S. Kim, and S. Kim, “Editsplat: Multi-view fusion and attention-guided optimization for view-consistent 3d scene editing with 3d gaussian splatting,” in *Proceedings of the Computer Vision and Pattern Recognition Conference*, 2025, pp. 11135–11145.
- [30] M. Chen, J. Xie, I. Laina, and A. Vedaldi, “Shap-editor: Instruction-guided latent 3d editing in seconds,” in *Proceedings of the IEEE/CVF Conference on Computer Vision and Pattern Recognition*, 2024, pp. 26456–26466.
- [31] Y. He, W. Yuan, S. Zhu, Z. Dong, L. Bo, and Q. Huang, “Freditor: High-fidelity and transferable nerf editing by frequency decomposition,” in *European Conference on Computer Vision*, 2024, pp. 73–91.
- [32] U. Khalid, H. Iqbal, N. Karim, M. Tayyab, J. Hua, and C. Chen, “Latenteditor: text driven local editing of 3d scenes,” in *European Conference on Computer Vision*, 2024, pp. 364–380.
- [33] Z. Shu, J. Yu, K. Chao, S. Xin, and L. Liu, “Gaussedit: Adaptive 3d scene editing with text and image prompts,” *IEEE Transactions on Visualization and Computer Graphics*, pp. 1–12, 2025.
- [34] R. He, S. Huang, X. Nie, T. Hui, L. Liu, J. Dai, J. Han, G. Li, and S. Liu, “Customize your nerf: Adaptive source driven 3d scene editing via local-global iterative training,” in *Proceedings of the IEEE/CVF conference on computer vision and pattern recognition*, 2024, pp. 6966–6975.
- [35] J.-K. Chen and Y.-X. Wang, “Proedit: Simple progression is all you need for high-quality 3d scene editing,” in *Advances in Neural Information Processing Systems*, vol. 37, 2024, pp. 4934–4955.
- [36] Y. Luo, S. Zhou, Y. Lan, X. Pan, and C. C. Loy, “3denhancer: Consistent multi-view diffusion for 3d enhancement,” in *Proceedings of the Computer Vision and Pattern Recognition Conference*, 2025, pp. 16430–16440.
- [37] Y. Cai, R. Li, and L. Liu, “Mv2mv: Multi-view image translation via view-consistent diffusion models,” *ACM Transactions on Graphics*, vol. 43, no. 6, pp. 1–12, 2024.
- [38] J.-K. Chen, S. R. Bulò, N. Müller, L. Porzi, P. Kotschieder, and Y.-X. Wang, “Consistdreamer: 3d-consistent 2d diffusion for high-fidelity scene editing,” in *Proceedings of the IEEE/CVF Conference on Computer Vision and Pattern Recognition*, 2024, pp. 21071–21080.
- [39] J. Wynn, Z. Qureshi, J. Powierza, J. Watson, and M. Sayed, “Morpheus: Text-driven 3d gaussian splat shape and color stylization,” in *Proceedings of the Computer Vision and Pattern Recognition Conference*, 2025, pp. 7825–7836.
- [40] J. Dong and Y.-X. Wang, “Vica-nerf: View-consistency-aware 3d editing of neural radiance fields,” *Advances in Neural Information Processing Systems*, vol. 36, 2024.
- [41] R. Liu, R. Wu, B. Van Hoorick, P. Tokmakov, S. Zakharov, and C. Vondrick, “Zero-1-to-3: Zero-shot one image to 3d object,” in *Proceedings of the IEEE/CVF international conference on computer vision*, 2023, pp. 9298–9309.
- [42] Y. Liu, C. Lin, Z. Zeng, X. Long, L. Liu, T. Komura, and W. Wang, “Syncdreamer: Generating multiview-consistent images from a single-view image,” in *The Twelfth International Conference on Learning Representations*, 2024.
- [43] Y. Shi, P. Wang, J. Ye, L. Mai, K. Li, and X. Yang, “MVDream: Multi-view diffusion for 3d generation,” in *The Twelfth International Conference on Learning Representations*, 2024.
- [44] P. Wang and Y. Shi, “Imagedream: Image-prompt multi-view diffusion for 3d generation,” *arXiv preprint arXiv:2312.02201*, 2023.
- [45] Z. Huang, H. Wen, J. Dong, Y. Wang, Y. Li, X. Chen, Y.-P. Cao, D. Liang, Y. Qiao, B. Dai *et al.*, “Epidiff: Enhancing multi-view synthesis via localized epipolar-constrained diffusion,” in *Proceedings of the IEEE/CVF Conference on Computer Vision and Pattern Recognition*, 2024, pp. 9784–9794.
- [46] Y. Kant, A. Siarohin, Z. Wu, M. Vasilkovsky, G. Qian, J. Ren, R. A. Guler, B. Ghanem, S. Tulyakov, and I. Gilitschenski, “Spad: Spatially aware multi-view diffusers,” in *Proceedings of the IEEE/CVF Conference on Computer Vision and Pattern Recognition*, 2024, pp. 10026–10038.
- [47] S. Tang, F. Zhang, J. Chen, P. Wang, and Y. Furukawa, “MVDiffusion: Enabling holistic multi-view image generation with correspondence-aware diffusion,” in *Thirty-seventh Conference on Neural Information Processing Systems*, 2023.
- [48] P. Li, Y. Liu, X. Long, F. Zhang, C. Lin, M. Li, X. Qi, S. Zhang, W. Xue, W. Luo *et al.*, “Era3d: high-resolution multiview diffusion using efficient row-wise attention,” *Advances in Neural Information Processing Systems*, vol. 37, pp. 55975–56000, 2024.
- [49] Z. Huang, Y.-C. Guo, H. Wang, R. Yi, L. Ma, Y.-P. Cao, and L. Sheng, “Mv-adapter: Multi-view consistent image generation made easy,” *arXiv preprint arXiv:2412.03632*, 2024.
- [50] X. Kong, S. Liu, X. Lyu, M. Taher, X. Qi, and A. J. Davison, “Eschnet: A generative model for scalable view synthesis,” in *Proceedings of the IEEE/CVF Conference on Computer Vision and Pattern Recognition*, 2024, pp. 9503–9513.
- [51] R. Rombach, A. Blattmann, D. Lorenz, P. Esser, and B. Ommer, “High-resolution image synthesis with latent diffusion models,” in *Proceedings of the IEEE/CVF conference on computer vision and pattern recognition*, 2022, pp. 10684–10695.
- [52] J. Song, C. Meng, and S. Ermon, “Denoising diffusion implicit models,” in *International Conference on Learning Representations*, 2021.
- [53] O. Ronneberger, P. Fischer, and T. Brox, “U-net: Convolutional networks for biomedical image segmentation,” in *MICCAI*, 2015, pp. 234–241.
- [54] A. Hertz, R. Mokady, J. Tenenbaum, K. Aberman, Y. Pritch, and D. Cohen-Or, “Prompt-to-prompt image editing with cross attention control,” *arXiv preprint arXiv:2208.01626*, 2022.
- [55] J. Xu, X. Liu, Y. Wu, Y. Tong, Q. Li, M. Ding, J. Tang, and Y. Dong, “Imagereward: Learning and evaluating human preferences for text-to-image generation,” *Advances in Neural Information Processing Systems*, vol. 36, pp. 15903–15935, 2023.
- [56] L. Tang, M. Jia, Q. Wang, C. P. Phoo, and B. Hariharan, “Emergent correspondence from image diffusion,” in *Thirty-seventh Conference on Neural Information Processing Systems*, 2023.
- [57] M. Tancik, E. Weber, E. Ng, R. Li, B. Yi, J. Kerr, T. Wang, A. Kristoffersen, J. Austin, K. Salahi, A. Ahuja, D. McAllister, and A. Kanazawa, “Nerfstudio: A modular framework for neural radiance field development,” in *ACM SIGGRAPH 2023 Conference Proceedings*, ser. SIGGRAPH ’23, 2023.
- [58] P. von Platen, S. Patil, A. Lozhkov, P. Cuenca, N. Lambert, K. Rasul, M. Davaadorj, D. Nair, S. Paul, W. Berman, Y. Xu, S. Liu, and T. Wolf, “Diffusers: State-of-the-art diffusion models,” <https://github.com/huggingface/diffusers>, 2022.
- [59] A. Kirillov, E. Mintun, N. Ravi, H. Mao, C. Rolland, L. Gustafson, T. Xiao, S. Whitehead, A. C. Berg, W.-Y. Lo *et al.*, “Segment anything,” in *Proceedings of the IEEE/CVF International Conference on Computer Vision*, 2023, pp. 4015–4026.
- [60] R. Zhang, P. Isola, A. A. Efros, E. Shechtman, and O. Wang, “The unreasonable effectiveness of deep features as a perceptual metric,” in *Proceedings of the IEEE conference on computer vision and pattern recognition*, 2018, pp. 586–595.
- [61] J. T. Barron, B. Mildenhall, D. Verbin, P. P. Srinivasan, and P. Hedman, “Mip-nerf 360: Unbounded anti-aliased neural radiance fields,” in *Proceedings of the IEEE/CVF Conference on Computer Vision and Pattern Recognition*, 2022, pp. 5470–5479.
- [62] Y. Yao, Z. Luo, S. Li, J. Zhang, Y. Ren, L. Zhou, T. Fang, and L. Quan, “Blendedmvs: A large-scale dataset for generalized multi-view stereo networks,” in *Proceedings of the IEEE/CVF conference on computer vision and pattern recognition*, 2020, pp. 1790–1799.
- [63] M. Asim, C. Wewer, T. Wimmer, B. Schiele, and J. E. Lenssen, “Met3r: Measuring multi-view consistency in generated images,” in *Proceedings of the Computer Vision and Pattern Recognition Conference*, 2025, pp. 6034–6044.
- [64] M. Oquab, T. Darcet, T. Moutakanni, H. Vo, M. Szafraniec, V. Khalidov, P. Fernandez, D. Haziza, F. Massa, A. El-Nouby *et al.*, “Dinov2:

Learning robust visual features without supervision," *Transactions on Machine Learning Research Journal*, pp. 1–31, 2024.